

Conforming and Nonconforming Virtual Element Methods for Signorini Problems

Yuping Zeng¹ · Liuqiang Zhong² · Mingchao Cai³ · Feng Wang⁴ · Shangyou Zhang⁵ ©

Received: 20 November 2023 / Revised: 20 March 2024 / Accepted: 6 May 2024

© The Author(s), under exclusive licence to Springer Science+Business Media, LLC, part of Springer Nature 2024

Abstract

In this paper, we design and analyze the conforming and nonconforming virtual element methods for the Signorini problem. Under some regularity assumptions, we prove optimal order a priori error estimates in the energy norm for both two numerical schemes. Extensive numerical tests are presented, verifying the theory and exploring unknown features.

Keywords Virtual element method · Conforming and nonconforming · Hexagonal mesh · Pentagonal mesh · Signorini problem · A priori error estimate

Mathematics Subject Classification 35J86 · 65N15 · 65N30

Shangyou Zhang szhang@udel.edu

Yuping Zeng zeng_yuping@163.com

Liuqiang Zhong zhong@scnu.edu.cn

Mingchao Cai cmchao2005@gmail.com

Published online: 03 June 2024

Feng Wang fwang@njnu.edu.cn

- School of Mathematics, Jiaying University, Meizhou 514015, China
- School of Mathematical Science, South China Normal University, Guangzhou 520631, China
- Department of Mathematics, Morgan State University, 1700 E Cold Spring Ln, Baltimore, MD 21251, USA
- Jiangsu Key Laboratory for NSLSCS, School of Mathematical Sciences, Nanjing Normal University, Nanjing 210023, China
- Department of Mathematical Sciences, University of Delaware, Newark, DE 19716, USA



1 Introduction

As a kind of classical nonlinear problem, variational inequalities (VIs) play an important role in mechanics, physics, engineering and management sciences. Their applications include contact between deformable bodies, the simulation of rolling wheels, elasticity membrane theory, antiplane frictional contact phenomenon, option pricing in financial mathematics. It is well know that elliptic VIs have two types. The first kind of VIs is featured by some closed convex set, while the second one is due to the presence of non-differentiable terms. Due to their variational properties, finite element methods (FEMs) are the mostly common used numerical schemes to approximate VIs. In this direction, we refer the reader to [9, 10, 14, 31, 32, 37, 42, 44, 59] for conforming FEMs, and to [24, 40, 43, 48, 49, 60] for nonconforming FEMs. However, the classical FEMs work only on simplicial meshes (see e.g., [12]). How to construct Galerkin scheme suitable for polygonal/polyhedra meshes is a hot topic in recent years. Among the attempts in this direction, virtual element method (VEM) is a successful paradigm, its main idea is to approximate partial differential equations by the usual polynomials plus some nonpolynomial functions. The objective of this work is to design and analysis conforming and nonconforming virtual element methods (VEMs) for the Signorini problem. For simplicity, we are concerned with the following scalar Signorini model:

$$-\Delta u = f \quad \text{in } \Omega,$$

$$u = 0 \quad \text{on } \Gamma_D,$$

$$\partial_n u = 0 \quad \text{on } \Gamma_N,$$

$$u > 0, \quad \partial_n u > 0, \quad u \partial_n u = 0 \quad \text{on } \Gamma_C,$$

$$(1)$$

where $\Omega \subset \mathbb{R}^2$ is a bounded polygonal domain with Lipschitz Γ that consists of three open disjoint parts, i.e., $\overline{\Gamma} = \overline{\Gamma_D} \cup \overline{\Gamma_N} \cup \overline{\Gamma_C}$ and $f \in L^2(\Omega)$. Here and in the following, we use the symbol $\partial_n u = \nabla u \cdot \boldsymbol{n}$, with \boldsymbol{n} being the outward unit normal vector.

History, VEM can be regarded as variational formulation of the mimetic finite difference (MFD). Its original principles and error analysis techniques can be traced back to [6], therein a conforming VEM is proposed for approximating the classical second order elliptic equation. The nonconforming version is developed in [4]. Later on, VEMs have been further extend to linear elasticity [8], Stokes equations [19, 26, 57, 61, 66], fourth order elliptic problems [2, 15, 64, 65], Darcy-Brinkman problems [20], Cahn-Hilliard equation [1], Biot's equations [17, 50], eigenvalue problems [35, 36], Laplace-Beltrami equation [34], fracture networks problems [11], interface problems [23]. The interesting works that deal with faces with arbitrarily small measure can be found in [7, 13, 16, 21, 22]. In the context of the approximation of VEM for VIs, there have existed some works on obstacle problems [54], simplified friction problem [33], Kirchhoff plate contact problem [56], Hemivariational inequality [55]. To the best of our knowledge, except for the work [53] wherein the linear conforming VEM is analyzed for contact problem on non-matching meshes, there exists no other work on VEMs for numerical approximation of Signorini problem. In the present work, we will make an further effort in this direction.

As mentioned above, designing Galerkin methods that allow for polygonal/polyhedra has received much attention in the last four decades. In the standard FEM framework, one can resorts to rational basics to construct polygonal/polyhedra discrete schemes. However, in this case, the construction of shape functions is highly challenging. On the other hand, alternative choices are interior penalty discontinuous Galerkin (IPDG) methods, which use totally discontinuous functions of piecewise polynomials on partition elements and rely on



18

some interior penalty techniques, and thus they have flexibility in handling of complicated geometries [3, 18]. For these reasons, IPDG method is also an effective numerical scheme for solving VIs (see e.g., [5, 16, 30, 39, 51, 52, 62] and the references therein). However, IPDG methods have more degrees of freedoms than classical FEMs on standard meshes. More recently, weak Galerkin (WG) method [38, 58] and hybrid high order (HHO) method [25, 27, 29], which featuring the discrete unknowns on mesh elements and faces, are also developed. In this work, we will focus on VEMs. In the space of VEMs, they choose functions as the solutions of some boundary value problem (which consist of the usual polynomials and additional nonpolynomial functions). Moreover, they take appropriate projections on the the polynomial subspace that are computable in terms of degrees of freedom. Therefore, we can implement VEM by using only necessary degrees of freedom. We also refer the interested reader to [46] for an unify study on VEM and HHO method. The objective of this paper is to design VEMs for the Signorini problem and provide a detailed convergence analysis. We will show that the numerical schemes have optimal convergence order in the energy norm assuming some regularity results. It is worth mention that, the main difficulties come from the inherent nonlinearity of VI and the complexity of bilinear of VEMs. Additionally, both conforming and nonconforming VEMs are addressed. Comparing with conforming case, the nonconforming one is more difficult in numerical analysis. The main reason behind this is that, in nonconforming case, the discrete convex set K_h^{nc} (see (47) below) is not a subspace of the continuous one (see (2) below), thus we need some more intricate techniques to obtain the corresponding error estimates.

The rest of our paper is organized as follows. In Sect. 2, we introduce some preliminary results and variational formulation of the Signorini problem. Next, in Sects. 3 and 4, the conforming and nonconforming VEMs are investigated for solving Signorini problem, and the detailed error estimates also accomplished. Some numerical results that show the optimal order error bound are presented in Sect. 5. Finally, in the last section, some conclusions are made.

2 Model Problem and Some Notation

We first introduce some notation. Given a bounded domain $\mathcal{D} \subset \mathbb{R}^2$, we use $W^{m,p}(\mathcal{D})(m > 0)$ to denote the standard Sobolev spaces, which consists of functions with derivatives of global order up to m in $L^p(D)$, and whose associated norm and seminorm are denoted by $\|\cdot\|_{m,p,\mathcal{D}}$ and $|\cdot|_{m,p,\mathcal{D}}$, respectively. When p=2, we use the notation $H^m(\Omega)=W^{m,2}(\Omega)$, in this case, we simply write its norm and seminorm as $\|\cdot\|_{m,\mathcal{D}}$ and $|\cdot|_{m,\mathcal{D}}$. We also define the inner product in $L^2(D)$ by $(w, v)_{\mathcal{D}} = \int_D wv dx$. In particular, $\mathcal{D} = \Omega$, we omit the index Ω .

Now, we introduce the space

$$V = \{ v \in H^1(\Omega) : v = 0 \text{ on } \Gamma_D \},$$

and the closed convex set

$$K = \{ v \in V : v \ge 0 \text{ on } \Gamma_C \}.$$
 (2)

It is well known that the variational formulation of the Signorini problem (1) reads: Find $u \in K$ such that (see [44])

$$a(u, v - u) > (f, v - u) \ \forall v \in K$$
.

where $a(u, v) = \int_{\Omega} \nabla u \cdot \nabla v dx$. In light of Stampacchia's theorem, this problem has a unique solution [45].



such that

3 The Conforming Virtual Element Method for Signorini Problem

3.1 The Conforming Virtual Element Method

Let \mathcal{T}_h be a family of meshes which decompose Ω into polygonal elements $\{T\}$. Set $h_T = \operatorname{diam}(T)$ and $h = \max_{T \in \mathcal{T}_h} h_T$. The set of interior edges is denote by \mathcal{E}_h^I . Similarly, the set of edges on Γ_D , Γ_N and Γ_C are denoted by \mathcal{E}_h^D , \mathcal{E}_h^N , and \mathcal{E}_h^C , respectively. Therefore, the set of all edges $\mathcal{E}_h = \mathcal{E}_h^I \cup \mathcal{E}_h^D \cup \mathcal{E}_h^N \cup \mathcal{E}_h^C$. Additionally, we define $\mathcal{E}_h^T = \{e \in \mathcal{E}_h | e \in \partial T\}$ as the collection of edges lying on the boundary of T. The length of each edge $e \in \mathcal{E}_h$ is denoted by h_e . Also, let \mathbb{V}_h denotes the collection of vertices ν of the mesh \mathcal{T}_h . For any element T, we set $\mathbb{V}_h^T = \{\nu \in \mathbb{V}_h : \nu \in \partial T\}$. The position of any vertex ν is denoted \mathbf{a}_{ν} . Furthermore, we assume that Γ_D , Γ_N and Γ_C are aligned with the triangulations \mathcal{T}_h , i.e., the end points of Γ_D and Γ_C coincide with the vertices of some elements. In addition, we introduce $P_k(\mathcal{D})$ to

denote the space of polynomials of degree at most k on \mathcal{D} . Inspired by [6], we also assume that the mesh \mathcal{T}_h satisfies some regularity conditions, that is, there exits a constant $\gamma > 0$,

A1: Every element T of \mathcal{T}_h is star-shaped with regard to a ball of radius of γh_T ;

A2: For every edge e of T, it satisfies $h_e \ge \gamma h_T$.

Following [6], we first introduce local P_k ($k \ge 1$) conforming VEM space as

$$V_h^c(T) = \{ v \in H^1(T) : \ \Delta v \in P_{k-2}(T), \ v|_{\partial T} \in B_k(\partial T) \}$$
 (3)

with boundary space $B_k(\partial T)$ defining by

$$B_k(\partial T) = \{ v \in C^0(\partial T) : v|_e \in P_k(e), \ \forall e \in \mathcal{E}_h^T \}.$$
 (4)

The associated degrees of freedom are

$$\chi_{i}(v_{h}) = v_{h}(\boldsymbol{a}_{i}) \quad \forall \boldsymbol{a}_{i} \in \mathbb{V}_{h}^{T},$$

$$\chi_{j}(v_{h}) = \int_{e} v_{h} p_{k-1} ds \quad \forall p_{k-2} \in P_{k-1}(e), \ e \in \mathcal{E}_{h}^{T},$$

$$\chi_{l}(v_{h}) = \int_{T} v_{h} p_{k-2} dx \quad \forall p_{k-2} \in P_{k-2}(T), \ T \in \mathcal{T}_{h}.$$

$$(5)$$

By the standard theory of VEM, we can prove that the above local space is unisolvent (see [6]). Also, using this local space, we take the global H^1 conforming VE space for problem (1) in the form

$$V_h^c = \left\{ v \in H_{\Gamma_D}^1(\Omega) : v|_T \in V_h^c(T), \ \forall T \in \mathcal{T}_h \right\}. \tag{6}$$

Usually, there exit singularities for the Signorini problem, one tends to use the lowest order P_1 VEM. Thus, for simple notations, we present the rest analysis only for k = 1 in (3). But the numerical computations are done for all k = 1 to 5.

We now recall the construction of bilinear forms of the conforming VEM. We begin by defining the projection operator $\Pi_T^c: V_h^c(T) \to P_1(T)$ as

$$a_T(\Pi_T^c v, q) = a_T(v, q) \quad \forall q \in P_1(T),$$

$$\overline{\Pi_T^c v} = \overline{v},$$
(7)



18

with

$$\overline{\psi} = \frac{1}{|\mathbb{V}_h^T|} \sum_{i=1}^{|\mathbb{V}_h^T|} \chi_i(\psi) = \frac{1}{|\mathbb{V}_h^T|} \sum_{i=1}^{|\mathbb{V}_h^T|} \psi(\boldsymbol{a}_i), \quad \boldsymbol{a}_i = \text{vertices of } T.$$
 (8)

Additionally, we choose the stabilized term as

$$S_T^c(u - \Pi_T^c u, v - \Pi_T^c v) = \sum_{i=1}^{|V_h^T|} \chi_i(u - \Pi_T^c u) \chi_i(v - \Pi_T^c v),$$

and define the bilinear form for each element T,

$$a_{h,T}^{c}(u,v) := a_{T}(\Pi_{T}^{c}u,\Pi_{T}^{c}v) + S_{T}^{c}(u - \Pi_{T}^{c}u,v - \Pi_{T}^{c}v).$$

Summing over all elements implies that

$$a_h^c(u, v) = \sum_{T \in \mathcal{T}_h} a_{h,T}^c(u, v).$$
 (9)

It is not difficult to check that the bilinear form satisfies the following consistency and stability properties.

B1 Polynomial consistency: Given $v_h \in V_h^c(T)$, it holds that

$$a_{h,T}^{c}(v_h, q) = a_T(v_h, q) \quad \forall q \in P_1(T).$$
 (10)

B2 Stablity: There exists two constants C_I and C_{II} , independent of h, such that

$$C_{l}a_{T}(v_{h}, v_{h}) \le a_{h,T}^{c}(v_{h}, v_{h}) \le C_{u}a_{T}(v_{h}, v_{h}) \quad \forall v_{h} \in V_{h}^{c}(T).$$
 (11)

We now give an approximation for the convex set K:

$$K_h^c = \{ v_h \in V_h^c : \chi_i(v_h) = v_h(a_i) \ge 0, \ i = 1, ..., |V_{\Gamma_C}| \},$$
 (12)

where $|\mathbb{V}_{\Gamma_C}|$ denotes the total number of degrees of freedom on Γ_C . Also, the corresponding right-hand term are approximated by

$$(f_h^c, v_h) = \sum_{T \in \mathcal{T}_h} \int_T (\mathbb{Q}_0^T f) \overline{v}_h dx, \tag{13}$$

where \mathbb{Q}_0^T is the standard L^2 projection onto $P_0(T)$, and \overline{v}_h can be understood from (8). The conforming VEM for (1) reads: Find $u_h^c \in K_h^c$ such that

$$a_h^c(u_h^c, v_h - u_h^c) \ge (f_h^c, v_h - u_h^c) \quad \forall v_h \in K_h^c.$$
 (14)

3.2 Error Estimates

This subsection aims at establishing a detailed a priori error estimate for the numerical scheme (14). To this end, we first recall the following trace inequality (see e.g., [28, 47])

$$h_e^{-1} \|w\|_{0,e}^2 \le C \left(h_T^{-2} \|w\|_{0,T}^2 + \|\nabla w\|_{0,T}^2 \right) \quad \forall w \in H^1(T), \tag{15}$$

with $e \in \mathcal{E}_h^T$. Here and throughout the paper, we utilize C to denote a positive generic constant that is independent of h, but may take different values at different occurrences.



In addition, for $v \in H^1(T) \cap C^0(\overline{T})$, we introduce the canonical interpolation $v_I \in V_h^c(T)$,

$$v_I(\boldsymbol{a}_i) = v(\boldsymbol{a}_i) \quad \forall \boldsymbol{a}_i \in \mathcal{V}_h^T.$$
 (16)

According to the assumptions A1 and A2, we have the following approximation results [6].

Lemma 3.1 It holds that

$$||v - v_I||_{0,T} + h_T |v - v_I|_{1,T} \le C h_T^2 |v|_{2,T}, \tag{17}$$

$$\inf_{q \in \Phi_h} |u - q|_{1,h} \le Ch|u|_2,\tag{18}$$

where
$$|w|_{1,h} = \left(\sum_{T \in \mathcal{T}_h} |w|_{1,T}^2\right)^{1/2}$$
 and $\Phi_h = \{v \in L^2(\Omega) : v|_T \in P_1(T)\}.$

Moreover, we establish an useful preliminary result, that is a key step to derive our final error bound.

Theorem 3.2 Let u and u_h^c denote the solutions of (1) and (14), respectively. Then, it holds that

$$|u - u_h^c|_1^2 \le C_a \Big\{ |u - u_I|_1^2 + \inf_{q \in \Phi_h} |u - q|_{1,h}^2 + \Theta_c^2 + \mathbb{R}_c \Big\}, \tag{19}$$

where $\mathbb{R}_{c} = a(u, u_{I} - u_{h}^{c}) - (f, u_{I} - u_{h}^{c})$, and

$$\Theta_{c} = \sup_{\substack{v_{h}^{c} \in V_{h}^{c} \\ v_{h}^{c} \neq 0}} \frac{|(f, v_{h}^{c}) - (f_{h}^{c}, v_{h}^{c})|}{|v_{h}^{c}|_{1}}.$$

Proof Applying the triangle inequality yields

$$|u - u_h^c|_1^2 \le (|u - u_I|_1 + |u_I - u_h^c|_1)^2$$

$$\le 2|u - u_I|_1^2 + 2|u_I - u_h^c|_1^2.$$
 (20)

Writing $z_h = u_I - u_h^c$, we conclude from (11) and (14) that

$$C_{l}|z_{h}|_{1,h}^{2} \leq a_{h}^{c}(z_{h}, z_{h}) = a_{h}^{c}(u_{I}, z_{h}) - a_{h}^{c}(u_{h}^{c}, z_{h}) \leq a_{h}^{c}(u_{I}, z_{h}) - (f_{h}^{c}, z_{h})$$

$$= \left[a_{h}^{c}(u_{I}, z_{h}) - a(u, z_{h})\right] + \left[a(u, z_{h}) - (f, z_{h})\right] + \left[(f, z_{h}) - (f_{h}^{c}, z_{h})\right]$$

$$\triangleq \mathbb{R}_{1} + \mathbb{R}_{c} + \mathbb{R}_{2},$$
(21)

for any $q \in \Phi_h$.

By adding and subtracting terms, we reformulate \mathbb{R}_1 as

$$\mathbb{R}_{1} = a_{h}^{c}(u_{I}, z_{h}) - a(u, z_{h})
= \sum_{T \in \mathcal{T}_{h}} \left[a_{h,T}^{c}(u_{I}, z_{h}) - a_{T}(u, z_{h}) \right]
= \sum_{T \in \mathcal{T}_{h}} \left[a_{h,T}^{c}(u_{I} - q, z_{h}) \right] + \left[a_{h,T}^{c}(q, z_{h}) - a_{T}(q, z_{h}) \right] + \left[a_{T}(q - u, z_{h}) \right]
\triangleq \mathbb{R}_{11} + \mathbb{R}_{12} + \mathbb{R}_{13}.$$
(22)



We combine (11) with Young's inequality to bound \mathbb{R}_{11} by

$$\mathbb{R}_{11} = \sum_{T \in \mathcal{T}_{h}} \left[a_{h,T}^{c}(u_{I} - q, z_{h}) \right] \\
\leq \sum_{T \in \mathcal{T}_{h}} C_{u} |u_{I} - q|_{1,T} |z_{h}|_{1,T} \\
\leq C_{u} |u_{I} - q|_{1,h} |z_{h}|_{1} \\
\leq C_{u} (|u - u_{I}|_{1} + |u - q|_{1,h}) |z_{h}|_{1} \\
\leq \frac{C_{u}^{2}}{4\epsilon_{1}} \left(|u - u_{I}|_{1} + |u - q|_{1,h} \right)^{2} + \epsilon_{1} |z_{h}|_{1}^{2} \\
\leq \frac{C_{u}^{2}}{2\epsilon_{1}} \left(|u - u_{I}|_{1}^{2} + |u - q|_{1,h}^{2} \right) + \epsilon_{1} |z_{h}|_{1}^{2}. \tag{23}$$

Due to the property of polynomial consistency stated in (10), the term \mathbb{R}_{12} satisfies

$$\mathbb{R}_{12} = \sum_{T \in \mathcal{T}_h} \left[a_{h,T}^c(q, z_h) - a_T(q, z_h) \right] = 0. \tag{24}$$

The continuity of each $a_T(\cdot, \cdot)$ implies that

$$\mathbb{R}_{13} = \sum_{T \in \mathcal{T}_h} \left[a_T(q - u, z_h) \right]
\leq \sum_{T \in \mathcal{T}_h} |u - q|_{1,T} |z_h|_{1,T}
\leq |u - q|_{1,h} |z_h|_1
\leq \frac{1}{4\epsilon_2} |u - q|_{1,h}^2 + \epsilon_2 |z_h|_1^2.$$
(25)

An immediate consequence of the definition of Θ_c shows that

$$\mathbb{R}_{2} = \left[(f, z_{h}) - (f_{h}^{c}, z_{h}) \right]$$

$$\leq \Theta_{c} |z_{h}|_{1}$$

$$\leq \frac{1}{4\epsilon_{3}} \Theta_{c}^{2} + \epsilon_{3} |z_{h}|_{1}^{2}.$$
(26)

Plugging the estimates (22)–(26) into (21), we claim that

$$\begin{aligned}
&\left(C_{l} - \epsilon_{1} - \epsilon_{2} - \epsilon_{3}\right) |z_{h}|_{1}^{2} \\
&\leq \frac{C_{u}}{2\epsilon_{1}} |u - u_{I}|_{1}^{2} + \left(\frac{C_{u}^{2}}{2\epsilon_{1}} + \frac{1}{4\epsilon_{2}}\right) |u - q|_{1,h}^{2} + \frac{1}{4\epsilon_{3}} \Theta_{c}^{2} + \mathbb{R}_{c}.
\end{aligned} (27)$$

Choose appropriate parameters ϵ_i (i=1,2,3) to satisfy $C_l - \epsilon_1 - \epsilon_2 - \epsilon_3 > 0$, this together with (20) yields the desired assertion.

Employing the above result, and adopting some techniques developed in [14], we can derive optimal order a priori error estimate in the energy norm.

Theorem 3.3 Let u and u_h^c be the solutions of (1) and (14), respectively. Assume that $u \in H^2(\Omega)$ and $\partial_n u|_{\Gamma_C} \in L^\infty(\Gamma_C)$, and the number of transition points from u = 0 and u > 0 on Γ_C is finite. Then we have

$$|u - u_h^c|_1 \le Ch. \tag{28}$$

Proof Our starting point is the estimate (19), we shall establish the contained terms step by step. From (17) and (18) we obtain

$$|u - u_I|_1 \le Ch|u|_2,$$
 (29)

$$\inf_{q \in \Phi_h} |u - q|_{1,h} \le Ch|u|_2. \tag{30}$$

Also, the approximation term satisfies (see [6])

$$|(f, v_h^c) - (f_h^c, v_h^c)| \le Ch|f|_{1,h}|v_h^c|_{1,h}$$

which leads to

$$\Theta_{c} = \sup_{\substack{v_{h}^{c} \in V_{h}^{c} \\ v_{f}^{c} \neq 0}} \frac{|(f, v_{h}^{c}) - (f_{h}^{c}, v_{h}^{c})|}{|v_{h}^{c}|_{1}} \le Ch|f|_{1,h}.$$
(31)

Thus, it remains to estimate $\mathbb{R}_c = a(u, u_I - u_h^c) - (f, u_I - u_h^c)$. Noting that $u_I - u_h^c = 0$ on Γ_D and $\partial_n u = 0$ on Γ_N , we apply integration by parts to obtain

$$\mathbb{R}_{c} = a(u, u_{I} - u_{h}^{c}) - (f, u_{I} - u_{h}^{c})
= \sum_{e \in \mathcal{E}_{h}^{C}} \int_{e} (\partial_{n} u)(u_{I} - u_{h}^{c}) ds.$$
(32)

By setting $\Gamma_C^0 = \{x \in \Gamma_C : u(x) = 0\}$ and $\Gamma_C^+ = \{x \in \Gamma_C : u(x) > 0\}$, we split the set of edges on \mathcal{E}_h^C into three disjoint subsets:

$$\begin{split} \Gamma_h^0 &= \{e \in \mathcal{E}_h^C : e \in \Gamma_C^0\}, \\ \Gamma_h^+ &= \{e \in \mathcal{E}_h^C : e \in \Gamma_C^+\}, \\ \Gamma_h^* &= \{e \in \mathcal{E}_h^C : e \cap \Gamma_C^0 \neq \emptyset, \ e \cap \Gamma_C^+ \neq \emptyset\}. \end{split}$$

Consequently,

$$\mathbb{R}_{c} = \sum_{e \in \mathcal{E}_{h}^{C}} \int_{e} (\partial_{n}u)(u_{I} - u_{h}^{c})ds$$

$$= \sum_{e \in \Gamma_{h}^{0}} \int_{e} (\partial_{n}u)(u_{I} - u_{h}^{c})ds + \sum_{e \in \Gamma_{h}^{+}} \int_{e} (\partial_{n}u)(u_{I} - u_{h}^{c})ds$$

$$+ \sum_{e \in \Gamma_{h}^{*}} \int_{e} (\partial_{n}u)(u_{I} - u_{h}^{c})ds$$

$$\leq \sum_{e \in \Gamma_{h}^{0}} \int_{e} (\partial_{n}u)(u_{I})ds + \sum_{e \in \Gamma_{h}^{+}} \int_{e} (\partial_{n}u)(u_{I})ds$$

$$+ \sum_{e \in \Gamma_{h}^{*}} \int_{e} (\partial_{n}u)(u_{I} - u)ds. \tag{33}$$

In the last step we have used the fact that $\partial_n u \geq 0$, $u_h^c \geq 0$ and $(\partial_n u)u = 0$ on Γ_C . We also emphasize that the edge e is understood as a closed set here and in the following, the reason behind is that the value of u at the end points that belong two adjacent edges need be treated carefully. For example, let e_1 and e_2 be two adjacent edges, suppose u=0 on e_1



(i.e., $e_1 \in \Gamma_h^0$), if u > 0 on $e_2 \setminus (e_1 \cap e_2)$, then $e_2 \in \Gamma_h^*$. We now deal with the above three terms in \mathbb{R}_c . If $e \in \Gamma_h^0$, since u = 0, this implies $u_1 = 0$, thus we have

$$\sum_{e \in \Gamma_h^0} \int_e (\partial_n u)(u_I) ds = 0. \tag{34}$$

If $e \in \Gamma_h^+$, since u > 0, this in conjunction with $(\partial_n u)u = 0$ leads to $(\partial_n u) = 0$, we infer

$$\sum_{e \in \Gamma_h^+} \int_e (\partial_n u)(u_I) ds = 0. \tag{35}$$

If $e \in \Gamma_h^*$, in light of (17) and the Cauchy-Schwarz inequality, we deduce that

(2024) 100:18

$$\int_{e} (\partial_{n} u)(u_{I} - u)ds \leq \|\partial_{n} u\|_{0,\infty,e} \int_{e} |u_{I} - u|ds
\leq C h_{e}^{1/2} \|\partial_{n} u\|_{0,\infty,e} \|u - u_{I}\|_{0,e}
\leq C h^{2} \|\partial_{n} u\|_{0,\infty,e} |u|_{2,T},$$
(36)

with $e \in \mathcal{E}_h^T$. Hence, summing over all edges $e \in \Gamma_h^*$ implies

$$\sum_{e \in \Gamma_h^*} \int_e (\partial_n u)(u_I - u) ds \le Ch^2 \|\partial_n u\|_{0,\infty,e} \sum_{e \in \Gamma_h^*} |u|_{2,T}$$

$$\le Ch^2 \|\partial_n u\|_{0,\infty,\Gamma_C} |u|_{2}. \tag{37}$$

In the last step, we have used the assumption that the number of transition points from u = 0 and u > 0 on Γ_C is finite.

Substituting (34), (35) and (37) into (33) yields

$$\mathbb{R}_{c} = \sum_{e \in \mathcal{E}_{h}^{C}} \int_{e} (\partial_{n} u)(u_{I} - u_{h}^{c}) ds$$

$$\leq C h^{2} \|\partial_{n} u\|_{0,\infty,\Gamma_{C}} |u|_{2}. \tag{38}$$

Finally, collecting the results (29)–(31) and (38), and inserting them into (19), we obtain the desired conclusion (28).

Remark 1 We stress that the estimate (19) in Theorem 3.2 can also be derived from Theorem 3.5 in [55] or the work [53]. In particular, a more general case that contains non-differential term has also been tackled in [55] and [53]. For completeness of the paper, we restate and prove (19) in detailed here, which is also useful to establish a similar bound for NVEM in the next section (see Theorem 4.2 below).

4 The Nonconforming Virtual Element Method for Signoroni Problem

4.1 The Nonconforming Virtual Element Method

In this section, we shall further explore the nonconforming VEM for the model problem (1). We first mention that, the mesh decomposition is analogous to the previous conforming case.



We then define the local P_k ($k \ge 1$) nonconforming VEM space as

$$V_h^{nc}(T) = \{ v \in H^1(T) : \Delta v \in P_{k-2}(T), \ \partial_n v|_e \in P_{k-1}(e), \ e \in \mathcal{E}_h^T \}.$$
 (39)

The associated degrees of freedom are

$$\chi_j(v_h) = \int_e v_h p_{k-1} ds \ \forall p_{k-1} \in P_{k-1}(e), e \in \mathcal{E}_h^T, \tag{40}$$

$$\chi_{l}(v_{h}) = \int_{T} v_{h} p_{k-2} dx \ \forall p_{k-2} \in P_{k-2}(T), T \in \mathcal{T}_{h}.$$
 (41)

The unisolvence of this local space has been shown in [4]. And the corresponding global nonconforming VEM space V_h^{nc} for problem (1) take the form

$$V_{h}^{nc} = \left\{ v \in L^{2}(\Omega) : \ v|_{T} \in V_{h}^{nc}(T), \ \int_{e} [v]_{e} p_{k-1} ds = 0, \ \forall e \in \mathcal{E}_{h}^{I} \cup \mathcal{E}_{h}^{D} \right\}, \tag{42}$$

where $[v]_e$ denotes the usual jump of v across the edge e, in particular, when $e \in \mathcal{E}_h^D$, $[v]_e = v$.

Again, as for the conforming elements, for simple notations, we provide the analysis for P_1 nonconforming VEM only, that is, k = 1 in (39). But the numerical computations are done for many high-order P_k nonconforming VEMs.

To state the bilinear form for the nonconforming VEM, we first introduce the projection operator $\Pi_T^{nc}: V_h^{nc}(T) \to P_1(T)$ as the solution of

$$a_T(\Pi_T^{nc}v, q) = a_T(v, q) \quad \forall q \in P_1(T),$$

$$\int_{\partial T} \Pi_T^{nc}v ds = \int_{\partial T} v ds.$$

By taking the choice

$$S_T^{nc}(u - \Pi_T^{nc}u, v - \Pi_T^{nc}v) = \sum_{e \in \mathcal{E}_h^T} \chi_e(u - \Pi_T^{nc}u) \chi_e(v - \Pi_T^{nc}v),$$

we define

$$a_{hT}^{nc}(u, v) = a_T(\Pi_T^{nc}u, \Pi_T^{nc}v) + S_T^{nc}(u - \Pi_T^{nc}u, v - \Pi_T^{nc}v).$$

Summing over all $T \in \mathcal{T}_h$ yields

$$a_h^{nc}(u,v) = \sum_{T \in \mathcal{T}_h} a_{h,T}^{nc}(u,v).$$
 (43)

Moreover, they satisfy the following polynomial consistency and stability properties [4].

C1 Polynomial consistency: Given $v_h \in V_h^{nc}(T)$, it satisfies

$$a_{h,T}^{nc}(v_h, q) = a_T(v_h, q) \quad \forall q \in P_1(T).$$
 (44)

C2 Stablity: It holds that

$$C_{\alpha}a_T(v_h, v_h) \le a_{h,T}^{nc}(v_h, v_h) \le C_{\beta}a_T(v_h, v_h) \quad \forall v_h \in V_h^{nc}(T). \tag{45}$$

The discrete approximation K_h^{nc} is formulated by

$$K_h^{nc} = \{ v_h \in V_h^{nc} : \chi_e(v_h) \ge 0, \quad \forall e \in \mathcal{E}_h^C \}.$$

$$\tag{46}$$



In this case, the right-hand approximation term is more involved than the conforming one. Inspired by [4], for each $T \in \mathcal{T}_h$, we first define

$$\tilde{v}_h = \frac{1}{3} \sum_{e \in \mathcal{E}_h^T} \int_e v_h ds,$$

and then set the approximation term as

$$(f_h^{nc}, v_h) = \sum_{T \in \mathcal{T}_h} \int_T (\mathbb{Q}_0 f) \tilde{v}_h dx.$$
 (47)

The nonconforming VEM for (1) reads: Find $u_h^{nc} \in K_h^{nc}$ satisfying

(2024) 100:18

$$a_h^{nc}(u_h^{nc}, v_h - u_h^{nc}) \ge (f_h^{nc}, v_h - u_h^{nc}) \quad \forall v_h \in K_h^{nc}.$$
 (48)

4.2 Error Estimates

To proceed, for $v \in H^1(T)$, we first define canonical interpolation $\Pi_h v \in V_h^{nc}(T)$ that satisfies

$$\chi_e(\Pi_h v) = \chi_e(v) \quad \forall e \in \mathcal{E}_h^T. \tag{49}$$

Under the assumptions A1 and A2, we have the following approximate properties [4].

Lemma 4.1 It holds that

$$||v - \Pi_h v||_{0,T} + h_T |v - \Pi_h v|_{1,T} \le C h_T^2 |v|_{2,T},$$
(50)

$$\inf_{q \in \Phi_h} |u - q|_{1,h} \le Ch|u|_2. \tag{51}$$

For nonconforming VEM, applying analogous techniques as in the conforming case in Theorem 3.3, we can obtain the following assertion.

Theorem 4.2 Let u and u_h^{nc} denote the solutions of (1) and (48), respectively. Then, it holds that

$$|u - u_h^{nc}|_{1,h}^2 \le C_b \Big\{ |u - \Pi_h u|_{1,h}^2 + \inf_{q \in \Phi_h} |u - q|_{1,h}^2 + \Theta_{nc}^2 + \mathbb{R}_{nc} \Big\},$$
 (52)

where $\mathbb{R}_{nc} = a_h^{nc}(u, \Pi_h u - u_h^{nc}) - (f, \Pi_h u - u_h^{nc})$, and

$$\Theta_{nc} = \sup_{\substack{v_h^{nc} \in V_h^{nc} \\ v_h^{nc} \neq 0}} \frac{|(f, v_h^{nc}) - (f_h^{nc}, v_h^{nc})|}{|v_h^{nc}|_{1,h}}.$$
 (53)

Proof As in (19) for the conforming case above, a similar formula holds for NVEM. More precisely, denote $z_h^{nc} = \Pi_h u - u_h^{nc}$, applying (45) and (48) to infer that

$$C_{\alpha}|z_{h}^{nc}|_{1,h}^{2} \leq a_{h}^{nc}(z_{h}^{nc}, z_{h}^{nc}) = a_{h}^{nc}(\Pi_{h}u, z_{h}^{nc}) - a_{h}^{nc}(u_{h}^{nc}, z_{h}^{nc})$$

$$\leq a_{h}^{nc}(\Pi_{h}u, z_{h}^{nc}) - (f_{h}^{nc}, z_{h}^{nc})$$

$$= \left[a_{h}^{nc}(\Pi_{h}u, z_{h}^{nc}) - a_{h}^{nc}(u, z_{h}^{nc})\right] + \left[a_{h}^{nc}(u, z_{h}^{nc}) - (f, z_{h}^{nc})\right]$$

$$+ \left[(f, z_{h}^{nc}) - (f_{h}^{nc}, z_{h}^{nc})\right] \triangleq \mathbb{R}_{1}^{nc} + \mathbb{R}_{nc} + \mathbb{R}_{2}^{nc}.$$
(54)

The assertion (53) follows by direct imitation of the proofs addressed in Theorem 3.3.



Next, to accomplish the final error estimate, we require the following preliminary result.

Lemma 4.3 Let u and u_h^{nc} be the solutions of (1) and (48), respectively. Assume that $u \in$ $H^2(\Omega)$, $u|_{\Gamma_C} \in W^{1,\infty}(\Gamma_C)$, and the number of transition points from u=0 and u>0 on Γ_C is finite, we have

$$-\sum_{e \in \Gamma_h^*} \int_e (\partial_n u) (u_h^{nc}) ds \le Ch |u|_2 |u - u_h^{nc}|_{1,h} + Ch^2 |u|_2 |u|_{1,\infty,\Gamma_C}.$$
 (55)

Proof Provide $e \in \Gamma_h^*$, we claim that $\partial_n u \geq 0$ and $\mathscr{P}_0^e(u_h^{nc}) = h_e^{-1} \int_{\mathscr{E}} u_h^{nc} ds \geq 0$, these facts implies

$$-\int_{e} (\partial_{n}u)(u_{h}^{nc})ds$$

$$\leq -\int_{e} (\partial_{n}u)(u_{h}^{nc} - \mathcal{P}_{0}^{e}(u_{h}^{nc}))ds$$

$$= -\int_{e} \left(\partial_{n}u - \mathcal{P}_{0}^{e}(\partial_{n}u)\right) \left(u_{h}^{nc} - \mathcal{P}_{0}^{e}(u_{h}^{nc})\right)ds$$

$$= -\int_{e} \left(\partial_{n}u - \mathcal{P}_{0}^{e}(\partial_{n}u)\right) \left(u_{h}^{nc} - \mathcal{P}_{0}^{e}(u_{h}^{nc}) - u + \mathcal{P}_{0}^{e}(u)\right)ds$$

$$-\int_{e} \left(\partial_{n}u - \mathcal{P}_{0}^{e}(\partial_{n}u)\right) \left(u\right)ds$$

$$\triangleq \mathbb{S}_{1} + \mathbb{S}_{2}.$$
(56)

Recall the standard estimate

$$\|v - \mathscr{P}_0^e(v)\|_{0,e} \le Ch_T^{1/2}|v|_{1,T},\tag{57}$$

and simply write $\mathscr{R}_0^e(v) = v - \mathscr{P}_0^e(v)$, thus,

$$\mathbb{S}_{1} = -\int_{e} \left(\mathscr{R}_{0}^{e}(\partial_{n}u) \right) \left(\mathscr{R}_{0}^{e}(u_{h}^{nc} - u) \right) ds
\leq \|\mathscr{R}_{0}^{e}(\partial_{n}u)\|_{0,e} \|\mathscr{R}_{0}^{e}(u - u_{h}^{nc})\|_{0,e}
\leq C h_{T}^{1/2} |u|_{2,T} h_{T}^{1/2} |u - u_{h}^{nc}|_{1,T}
= C h_{T} |u|_{2,T} |u - u_{h}^{nc}|_{1,T}.$$
(58)

Since $e \in \Gamma_h^*$, there exits some Q_e satisfying $u(Q_e) = 0$, thus from 1D Poincaré's inequality (see e.g., [43]) we have $||u||_{0,e} \le Ch_e \left\| \frac{\partial u}{\partial s} \right\|_{0,e}$, this together (57) implies that

$$S_{2} = -\int_{e} \left(\mathscr{R}_{0}^{e}(\partial_{n}u) \right) \left(u \right) ds$$

$$\leq \| \mathscr{R}_{0}^{e}(\partial_{n}u) \|_{0,e} \| u \|_{0,e}$$

$$\leq C h_{T}^{1/2} |u|_{2,T} \| u \|_{0,e}$$

$$\leq C h_{T}^{1/2} h_{e} |u|_{2,T} \left\| \frac{\partial u}{\partial s} \right\|_{0,e}.$$
(59)

Moreover, we have

$$\left\| \frac{\partial u}{\partial s} \right\|_{0,e}^{2} \le C h_{e} \left\| \frac{\partial u}{\partial s} \right\|_{0,\infty,e}^{2} \le C h_{e} |u|_{1,\infty,\Gamma_{C}}^{2}. \tag{60}$$



Inserting (60) into (59), we arrive at

$$\mathbb{S}_2 \le C h_T^{1/2} h_e^{3/2} |u|_{2,T} u|_{1,\infty,\Gamma_C} \le C h^2 |u|_{2,T} |u|_{1,\infty,\Gamma_C}. \tag{61}$$

Collecting the estimates (58) and (61), summing over all $e \in \Gamma_h^*$, and utilizing the assumption that the number of transition points is finite, we infer that

$$-\sum_{e \in \Gamma_{h}^{*}} \int_{e} (\partial_{n} u)(u_{h}^{nc}) ds$$

$$\leq C \sum_{e \in \Gamma_{h}^{*}} \left(h_{T} |u|_{2,T} |u - u_{h}^{nc}|_{1,T} + h^{2} |u|_{2,T} |u|_{1,\infty,\Gamma_{C}} \right)$$

$$\leq C h |u|_{2} |u - u_{h}^{nc}|_{1,h} + h^{2} |u|_{2} |u|_{1,\infty,\Gamma_{C}}, \tag{62}$$

which is the assertion (55) as required.

We are now in a position to state the error analysis for the NVEM (48).

Theorem 4.4 Under the same assumptions in Lemma 4.3, there holds that

$$|u - u_h^{nc}|_{1,h} \le Ch. (63)$$

Proof It is enough to give estimates for all terms appear in (52). From (50) and (51), the first two terms satisfy

$$|u - \Pi_h u|_{1,h} \le Ch|u|_2,\tag{64}$$

$$\inf_{q \in \Phi_h} |u - q|_{1,h} \le Ch|u|_2. \tag{65}$$

Additionally, it can be proved that the approximation term satisfies (see [4])

$$|(f, v_h^{nc}) - (f_h^{nc}, v_h^{nc})| \le ch \|f\|_0 |v_h^{nc}|_{1,h},$$

this yields

$$\Theta_{nc} = \sup_{\substack{v_h^c \in V_{nc}^{nc} \\ v_h^{nc} \neq 0}} \frac{|(f, v_h^{nc}) - (f_h^{nc}, v_h^{nc})|}{|v_h^{nc}|_{1,h}} \le ch \|f\|_0.$$
 (66)

Thus, it leaves us to estimate $\mathbb{R}_{nc} = a(u, \Pi_h u - u_h^{nc}) - (f, \Pi_h u - u_h^{nc})$. By setting $w_h = \Pi_h u - u_h^{nc}$ and integrating by parts, we obtain

$$\mathbb{R}_{nc} = a(u, w_h) - (f, w_h)
= \sum_{T \in \mathcal{T}_h} \sum_{e \in \partial T} \int_{e} (\partial_n u)(w_h) ds
= \sum_{T \in \mathcal{T}_h} \sum_{e \in \partial T \setminus (\mathcal{E}_h^N \cup \mathcal{E}_h^C)} \int_{e} (\partial_n u)(w_h) ds + \sum_{e \in \mathcal{E}_h^N} \int_{e} (\partial_n u)(w_h) ds
+ \sum_{e \in \mathcal{E}_h^C} \int_{e} (\partial_n u)(w_h) ds
= \sum_{T \in \mathcal{T}_h} \sum_{e \in \partial T \setminus (\mathcal{E}_h^N \cup \mathcal{E}_h^C)} \int_{e} (\partial_n u)(w_h) ds + \sum_{e \in \mathcal{E}_h^C} \int_{e} (\partial_n u)(w_h) ds
\triangleq \mathbb{A}_1 + \mathbb{A}_2$$
(67)



The consistency error term \mathbb{A}_1 can be estimated by applying standard techniques for the NVEM and (57):

$$\mathbb{A}_{1} = \sum_{T \in \mathcal{T}_{h}} \sum_{e \in \partial T \setminus (\mathcal{E}_{h}^{N} \cup \mathcal{E}_{h}^{C})} \int_{e} (\partial_{n}u)(w_{h}) ds$$

$$= \sum_{T \in \mathcal{T}_{h}} \sum_{e \in \partial T \setminus (\mathcal{E}_{h}^{N} \cup \mathcal{E}_{h}^{C})} \int_{e} (\partial_{n}u - \mathscr{P}_{0}^{e}(\partial_{n}u)) \cdot (w_{h} - \mathscr{P}_{0}^{e}w_{h}) ds$$

$$\leq \sum_{T \in \mathcal{T}_{h}} \sum_{e \in \partial T \setminus (\mathcal{E}_{h}^{N} \cup \mathcal{E}_{h}^{C})} \|\partial_{n}u - \mathscr{P}_{0}^{e}(\partial_{n}u)\|_{0,e} \|w_{h} - \mathscr{P}_{0}^{e}w_{h}\|_{0,e}$$

$$\leq \sum_{T \in \mathcal{T}_{h}} Ch_{T}^{1/2} |u|_{2,T} h_{T}^{1/2} |w_{h}|_{1,T}$$

$$\leq Ch \left(\sum_{T \in \mathcal{T}_{h}} |u|_{2,T}^{2} \sum_{T \in \mathcal{T}_{h}} |w_{h}|_{1,T}^{2}\right)^{1/2}$$

$$\leq Ch |u|_{2} |\Pi_{h}u - u_{h}^{nc}|_{1,h}.$$
(68)

For \mathbb{A}_2 , we split it as

$$\mathbb{A}_{2} = \sum_{e \in \mathcal{E}_{h}^{C}} \int_{e} (\partial_{n}u)(\Pi_{h}u - u_{h}^{nc})ds$$

$$= \sum_{e \in \Gamma_{h}^{0}} \int_{e} (\partial_{n}u)(\Pi_{h}u - u_{h}^{nc})ds + \sum_{e \in \Gamma_{h}^{*}} \int_{e} (\partial_{n}u)(\Pi_{h}u - u_{h}^{nc})ds$$

$$= \sum_{e \in \Gamma_{h}^{0}} \int_{e} (\partial_{n}u)(\Pi_{h}u - u_{h}^{nc})ds + \sum_{e \in \Gamma_{h}^{*}} \int_{e} (\partial_{n}u)(\Pi_{h}u - u)ds$$

$$- \sum_{e \in \Gamma_{h}^{*}} \int_{e} (\partial_{n}u)(u_{h}^{nc})ds$$

$$\triangleq \mathbb{A}_{21} + \mathbb{A}_{22} + \mathbb{A}_{23}.$$
(69)

If $e \in \Gamma_h^0$, noting that u = 0 implies $\Pi_h u = 0$, $\int_e (u_h^{nc})(\mathscr{P}_0^e(\partial_n u))ds \ge 0$ (since $u_h^{nc} \in K_h^{nc}$) yields $\int_e (u_h^{nc})(\partial_n u)ds \ge \int_e (u_h^{nc})(\mathscr{R}_0^e(\partial_n u))ds$, these facts together with (57) yield

$$\int_{e} (\partial_{n}u)(\Pi_{h}u - u_{h}^{nc})ds \leq \int_{e} \mathscr{R}_{0}^{e}(\partial_{n}u)(\Pi_{h}u - u_{h}^{nc})ds
= \int_{e} \mathscr{R}_{0}^{e}(\partial_{n}u)(\Pi_{h}u - u)ds + \int_{e} \mathscr{R}_{0}^{e}(\partial_{n}u)\mathscr{R}_{0}^{e}(u - u_{h}^{nc})ds
\leq \|\mathscr{R}_{0}^{e}(\partial_{n}u)\|_{0,e} \Big(\|\Pi_{h}u - u\|_{0,e} + \|\mathscr{R}_{0}^{e}(u - u_{h}^{nc})\|_{0,e} \Big)
\leq Ch_{T}^{1/2}|u|_{2,T} \Big(h_{T}^{3/2}|u|_{2,T} + h_{T}^{1/2}|u - u_{h}^{nc}|_{1,T} \Big)
\leq Ch_{T}^{2}|u|_{2,T}^{2} + Ch_{T}|u|_{2,T}|u - u_{h}^{nc}|_{1,T}.$$
(70)

Summing over all $e \in \Gamma_h^0$, we obtain

$$\mathbb{A}_{21} \le Ch^2 |u|_2^2 + Ch|u|_2 |u - u_h^{nc}|_{1,h}. \tag{71}$$



In view of (50) and the Cauchy-Schwarz inequality, we claim that, for any $e \in \Gamma_h^*$,

$$\int_{e} (\partial_{n} u)(\Pi_{h} u - u) ds \leq \|\partial_{n} u\|_{0,\infty,e} \int_{e} |\Pi_{h} u - u| ds
\leq C h_{e}^{1/2} \|\partial_{n} u\|_{0,\infty,e} \|u - \Pi_{h} u\|_{0,e}
\leq C h^{2} \|\partial_{n} u\|_{0,\infty,e} |u|_{2,T},$$

with $e \in \mathcal{E}_h^T$. Summing over all edges $e \in \Gamma_h^*$ yields

$$\mathbb{A}_{22} = \sum_{e \in \Gamma_h^*} \int_e (\partial_n u) (\Pi_h u - u) ds$$

$$\leq Ch^2 \|\partial_n u\|_{0,\infty,\Gamma_C} \sum_{e \in \Gamma_h^*} |u|_{2,T}$$

$$\leq Ch^2 \|\partial_n u\|_{0,\infty,\Gamma_C} |u|_{2}.$$
(72)

In the last line, we have used the assumption that the number of transition points is finite.

For the term \mathbb{A}_{23} , it follows from Lemma 4.3 that

$$\mathbb{A}_{23} \le Ch|u|_2|u - u_h^{nc}|_{1,h} + Ch^2|u|_2|u|_{1,\infty,\Gamma_C}. \tag{73}$$

Substituting (68), (71)–(73) into (67), and applying the triangle and Young's inequalities yields

$$\mathbb{R}_{nc} \leq C_{1}h|u|_{2}|\Pi_{h}u - u_{h}^{nc}|_{1,h} + C_{2}h|u|_{2}|u - u_{h}^{nc}|_{1,h} + C_{3}h^{2}|u|_{2}^{2}
+ C_{4}h^{2}|u|_{2}|u|_{1,\infty,\Gamma_{C}}
\leq \frac{C_{1}^{2}}{4\epsilon_{4}}h^{2}|u|_{2}^{2} + \epsilon_{4}|\Pi_{h}u - u_{h}^{nc}|_{1,h}^{2} + \epsilon_{5}|u - u_{h}^{nc}|_{1,h}^{2} + \frac{C_{2}^{2}}{4\epsilon_{5}}h^{2}|u|_{2}^{2}
+ C_{3}h^{2}|u|_{2}^{2} + C_{4}h^{2}|u|_{2}|u|_{1,\infty,\Gamma_{C}}
\leq \frac{C_{1}^{2}}{4\epsilon_{4}}h^{2}|u|_{2}^{2} + 2\epsilon_{4}|u - u_{h}^{nc}|_{1,h}^{2} + 2\epsilon_{4}|u - \Pi_{h}u|_{1,h}^{2}
+ \epsilon_{5}|u - u_{h}^{nc}|_{1,h}^{2} + \frac{C_{2}^{2}}{4\epsilon_{5}}h^{2}|u|_{2}^{2} + C_{3}h^{2}|u|_{2}^{2} + C_{4}h^{2}|u|_{2}|u|_{1,\infty,\Gamma_{C}}. \tag{74}$$

We combine (52) with (74) to infer that

$$\left(1 - 2C_{b}\epsilon_{4} - C_{b}\epsilon_{5}\right)|u - u_{h}^{nc}|_{1,h}^{2}$$

$$\leq (C_{b} + 2\epsilon_{4})|u - \Pi_{h}u|_{1,h}^{2} + C_{b}\inf_{q\in\Phi_{h}}|u - q|_{1,h}^{2} + C_{b}\Theta_{nc}^{2}$$

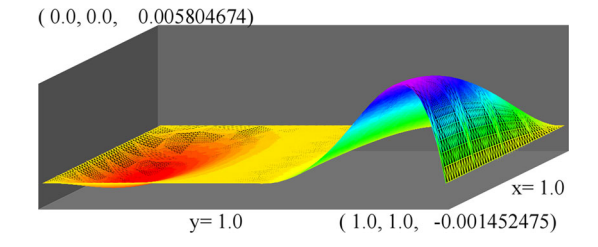
$$+ \left(\frac{C_{1}^{2}}{4\epsilon_{4}}h^{2} + \frac{C_{2}^{2}}{4\epsilon_{5}}h^{2} + C_{3}h^{2}\right)|u|_{2}^{2} + C_{4}h^{2}|u|_{2}|u|_{1,\infty,\Gamma_{C}}.$$
(75)

By choosing that $1 - 2C_b\epsilon_4 - C_b\epsilon_5 > 0$, and collecting results in (64)–(66) implies the desired estimate (63).

Remark 2 Comparing with the conforming VEM, to obtain optimal order error estimates, more stringent regularity assumptions on the exact solution are required in the analysis of nonconforming case. More precisely, for conforming VEM, it is assumed that $u \in H^2(\Omega)$ and $\partial_n u|_{\Gamma_C} \in L^\infty(\Gamma_C)$, while for nonconforming VEM, the assumption is that $u \in H^2(\Omega)$ and $u|_{\Gamma_C} \in W^{1,\infty}(\Gamma_C)$.



Fig. 1 The computed P_4 VEM solution on Grid 3 of Fig. 2 for problem (76) with an exact solution (77)



(2024) 100:18

5 Numerical Experiments

In this section, we provide some numerical results to validate the effectiveness of the VEMs. We solve the following Signorini problem:

$$-\Delta u = f \quad \text{in } \Omega,$$

$$u = 0 \quad \text{on } \Gamma_D,$$

$$u \partial_n u = 0, \ u \ge 0, \partial_n u \ge 0, \quad \text{on } \Gamma_C,$$

$$(76)$$

where $\Omega = (0, 1) \times (0, 1)$, $\Gamma_C = [0, 1] \times \{1\}$, $\Gamma_D = \partial \Omega \setminus \Gamma_C$.

When we choose the right-hand side function in (76) as

$$f = \frac{1 - 2x}{4} (4x^4 + 40x^2y^2 - 8x^3 - 40xy^2 + 5x^2 + 7y^2 - x + f_1),$$
where $f_1 = \begin{cases} -40x^2y + 40xy - 7y, & \text{if } x \le 1/2, \\ -80x^2y + 80xy - 14y, & \text{if } x > 1/2, \end{cases}$

we would get the exact solution u of (76) as

$$u = x(1-x)\left(x - \frac{1}{2}\right)^{3} y u_{1},$$
where $u_{1} =\begin{cases} 1 - y, & \text{if } x \leq 1/2, \\ 2 - y, & \text{if } x > 1/2. \end{cases}$ (77)

To view the solution, in Fig. 1, we plot the P_4 conforming VEM solution (k = 4 in (3)) on hexagonal Grid 3 (shown in Fig. 2). On the front left boundary, u = 0 and $\partial_n u > 0$. On the front right boundary, u > 0 and $\partial_n u = 0$.

To solve each nonlinear VEM equation, we apply the monotonic iteration method as follows (see [41]). Initially, we let

$$\Gamma_{C,D}^{(0)} = \emptyset$$
 and $\Gamma_{C,N}^{(0)} = \Gamma_C \setminus \Gamma_{C,D}^{(0)}$.

This way, in the m step, we separate the boundary condition $u\partial_n u = 0$ on Γ_C into two boundary conditions,

$$u|_{\Gamma_{C,N}^{(m)}} = 0 \text{ and } \partial_n u|_{\Gamma_{C,N}^{(m)}} = 0.$$
 (78)

With the linear boundary conditions (78), we have a unique VEM solution $u_h^{(m)}$ for the resulting discrete linear system of equation. To do next iteration, we update the boundary



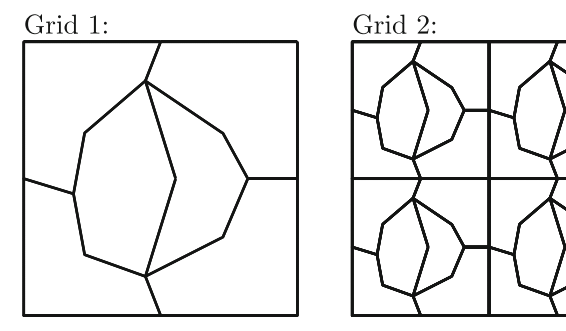


Fig. 2 The first two levels of hexagonal grids for the computation in Tables 1–8

Table 1 The error profile for (77) on meshes shown in Fig. 2, by the P_1 conforming VEM

Grid	$ u - u_h _0$	$O(h^r)$	$\ \nabla(u-u_h)\ _0$	$O(h^r)$	#Iter
1	0.5241E-02	0.00	0.2209E-01	0.00	1
2	0.1371E-02	1.93	0.7076E-02	1.64	1
3	0.3120E-03	2.14	0.2938E-02	1.27	1
4	0.1117E-03	1.48	0.1671E-02	0.81	1
5	0.2075E-04	2.43	0.7746E-03	1.11	2
6	0.5006E-05	2.05	0.3869E-03	1.00	2
7	0.1117E-05	2.16	0.1966E-03	0.98	5
8	0.2674E-06	2.06	0.9916E-04	0.99	6

conditions first by letting

$$\Gamma_{C,D}^{(m+1)} = \left(\Gamma_{C,D}^{(m)} \setminus \{e \in \Gamma_{C,D}^{(m)} : u(e_1) < 0 \& u(e_2) < 0\}\right)$$

$$\bigcup \left(\Gamma_{C,N}^{(m)} \setminus \{e \in \Gamma_{C,N}^{(m)} : \partial_n u(e_1) < 0 \& \partial_n u(e_2) < 0\}\right),$$

$$\Gamma_{C,N}^{(m+1)} = \Gamma_C \setminus \Gamma_{C,D}^{(m+1)},$$

where e_1 and e_2 are the two end points of an edge e on the boundary Γ_C . The iteration is stopped when

$$\Gamma_{C,D}^{(m+1)} = \Gamma_{C,D}^{(m)} = \Gamma_{C,D}^{(m-1)}.$$
(79)

There is no other choice because when the iteration reaches the status (79), the solution $u_h^{(m+1)} = u_h^{(m)}$ and remains the same for ever.

In Table 1, the results for the P_1 conforming VEM approximating solution (77) are listed, where #Iter is the number of monotonic iterations (78)–(79) performed. The P_1 conforming VEM converges at the optimal order in both norms.

In Table 2, we compute the P_2 conforming VEM solutions for (77) on the hexagonal meshes shown in Fig. 2. The P_2 conforming VEM converges at the optimal order in both norms.

In Table 3, we compute the P_3 conforming VEM solutions for (77) on the hexagonal meshes shown in Fig. 2. The P_3 conforming VEM converges at the optimal order in H^1 -norm. But it seems we have an half order sub-optimal convergence in L^2 -norm. Since the exact solution (77) is in $H^{3.5-\epsilon}(\Omega)$, this would explain somewhat the sub-optimal convergence. See



18

Grid	$ u - u_h _0$	$O(h^r)$	$\ \nabla(u-u_h)\ _0$	$O(h^r)$	# Iter
1	0.1475E-02	0.00	0.1770E-01	0.00	1
2	0.2260E-03	2.71	0.5150E-02	1.78	1
3	0.2727E-04	3.05	0.1270E-02	2.02	3
4	0.2865E-05	3.25	0.3056E-03	2.05	3
5	0.4365E-06	2.71	0.7546E-04	2.02	6
6	0.4878E-07	3.16	0.1867E-04	2.01	10
7	0.5687E-08	3.10	0.4649E-05	2.01	12

Table 3 The error profile for (77) on meshes shown in Fig. 2, by the P_3 conforming VEM

Grid	$ u-u_h _0$	$O(h^r)$	$\ \nabla (u-u_h)\ _0$	$O(h^r)$	# Iter
1	0.3198E-02	0.00	0.2711E-01	0.00	1
2	0.1669E-03	4.26	0.3291E-02	3.04	1
3	0.6540E-05	4.67	0.3719E-03	3.15	3
4	0.2740E-05	1.26	0.6631E-04	2.49	4
5	0.2488E-06	3.46	0.8240E-05	3.01	7
6	0.2223E-07	3.48	0.1025E-05	3.01	10

Table 4 The error profile for (77) on meshes shown in Fig. 2, by the P_4 conforming VEM

Grid	$\ u-u_h\ _0$	$O(h^r)$	$\ \nabla (u-u_h)\ _0$	$O(h^r)$	# Iter
1	0.7697E-02	0.00	0.4663E-01	0.00	1
2	0.2718E-04	8.15	0.7935E-03	5.88	3
3	0.4273E-05	2.67	0.8688E-04	3.19	3
4	0.2621E-05	0.71	0.4745E-04	0.87	4
5	0.2389E-06	3.46	0.5948E-05	3.00	6
6	0.2138E-07	3.48	0.7429E-06	3.00	9

Table 5 The error profile for (77) on meshes shown in Fig. 2, by the P_5 conforming VEM

Grid	$\ u-u_h\ _0$	$O(h^r)$	$\ \nabla (u-u_h)\ _0$	$O(h^r)$	# Iter
1	0.5289E-01	0.00	0.2597E+00	0.00	1
2	0.1252E-03	8.72	0.8973E-03	8.18	1
3	0.2007E-05	5.96	0.3729E-04	4.59	3
4	0.1574E-05	0.35	0.3024E-04	0.30	5
5	0.1426E-06	3.46	0.3788E-05	3.00	7
6	0.1273E-07	3.49	0.4731E-06	3.00	10

the comments on the P_4 and P_5 conforming VEM below, and the comments for computing the second example.

In Tables 4 and 5, we compute the P_4 and P_5 conforming VEM solutions, respectively, for (77) on the hexagonal meshes shown in Fig. 2. It is surprising and understandable that their convergence orders are exactly same as those of the P_3 conforming VEM in Table 3. There is no need to increase the order of VEM if the exact solution is not that smooth. We can see below in the second example that the convergence order of P_4 and P_5 can be higher.



Table 6 The error profile for (77) on meshes shown in Fig. 2, by the P_1 nonconforming VEM

Grid	$ u-u_h _0$	$O(h^r)$	$\ \nabla_h(u-u_h)\ _0$	$O(h^r)$	# Iter
1	0.2362E-02	0.00	0.1337E-01	0.00	1
2	0.4874E-03	2.28	0.4826E-02	1.47	1
3	0.1416E-03	1.78	0.2326E-02	1.05	1
4	0.1144E-03	0.31	0.1391E-02	0.74	1
5	0.1515E-04	2.92	0.5689E-03	1.29	2
6	0.2004E-05	2.92	0.2754E-03	1.05	2
7	0.4279E-06	2.23	0.1384E-03	0.99	3
8	0.1015E-06	2.08	0.6920E-04	1.00	8

Table 7 The error profile for (77) on meshes shown in Fig. 2, by the P_2 nonconforming VEM

Grid	$\ u-u_h\ _0$	$O(h^r)$	$\ \nabla_h(u-u_h)\ _0$	$O(h^r)$	# Iter
1	0.1475E-02	0.00	0.1770E-01	0.00	2
2	0.2260E-03	2.71	0.5150E-02	1.78	2
3	0.2727E-04	3.05	0.1270E-02	2.02	3
4	0.2865E-05	3.25	0.3056E-03	2.05	3
5	0.3461E-06	3.05	0.7517E-04	2.02	8
6	0.4878E-07	2.83	0.1867E-04	2.01	10
7	0.5687E-08	3.10	0.4649E-05	2.01	12

In Table 6, we report the results of computing solution (77) by P_1 nonconforming VEM on meshes shown in Fig. 2. Comparing to Table 1, the P_1 nonconforming VEM converges at the same order as the P_1 conforming VEM but with smaller errors as we have more degrees of freedom in the nonconforming VEM.

In Table 7, we compute the P_2 nonconforming VEM solutions for (77) on the hexagonal meshes shown in Fig. 2. The P_2 nonconforming VEM converges at the optimal order in both norms. However, comparing to Table 2, it seems that the extra five degrees of freedom on each hexagon do not provide any additional approximation, as the two methods produce almost identical results.

In Table 8, we compute the P_3 nonconforming VEM solutions for (77) on the hexagonal meshes shown in Fig. 2. The P_3 nonconforming VEM converges at the optimal order in both norms. It is quite surprising recalling that the P_3 conforming VEM converges half an order sub-optimal in L^2 -norm. We think, the designed discontinuous VEM P_3 solutions can stop the L^2 -error pollution near the jump point of the free boundary condition. For example, it is proved in [63] that the nonconforming element solution converges independently of the coefficient jump in solving an interface problem while the continuous finite element has an error bound of $a_{\rm max}/a_{\rm min}$ times that of error bound of the nonconforming element, where $a_{\rm max}$ and $a_{\rm min}$ are the maximum and the minimum of the diffusion coefficient of a 2nd order elliptic equation, respectively.

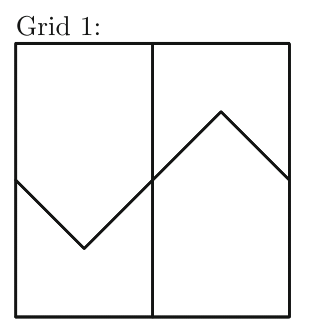
Next we test the VEM on pentagonal meshes shown in Fig. 3.

In Table 9, we compute the P_1 conforming VEM solutions for (77) on the pentagonal meshes shown in Fig. 3. The P_1 conforming VEM converges at the optimal order in both norms. Comparing to Table 1, we have less degrees of freedom in the pentagonal VEM than that of the hexagonal VEM. But the pentagonal meshes are more regular. It turns out the two methods are almost same in solving the Signorini problems.



Table 8 The error profile for (77) on meshes shown in Fig. 2, by the P_3 nonconforming VEM

Grid	$ u-u_h _0$	$O(h^r)$	$\ \nabla_h(u-u_h)\ _0$	$O(h^r)$	# Iter
1	0.3226E-02	0.00	0.2734E-01	0.00	1
2	0.1673E-03	4.27	0.3320E-02	3.04	1
3	0.6429E-05	4.70	0.3757E-03	3.14	2
4	0.3854E-06	4.06	0.4539E-04	3.05	4
5	0.2356E-07	4.03	0.5571E-05	3.03	7
6	0.1455E-08	4.02	0.6898E-06	3.01	10



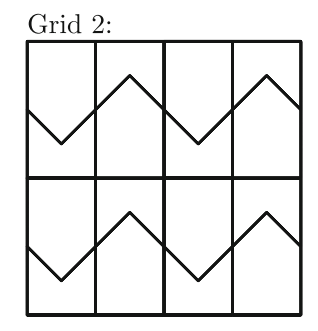


Fig. 3 The first two levels of pentagonal grids for the computation in Tables 9–14

Table 9 The error profile for (77) on meshes shown in Fig. 3, by the P_1 conforming VEM

Grid	$ u - u_h _0$	$O(h^r)$	$\ \nabla_h(u-u_h)\ _0$	$O(h^r)$	# Iter
1	0.4850E-02	0.00	0.1978E-01	0.00	1
2	0.1815E-02	1.42	0.8994E-02	1.14	1
3	0.4452E-03	2.03	0.3475E-02	1.37	1
4	0.1245E-03	1.84	0.1685E-02	1.04	1
5	0.2547E-04	2.29	0.7306E-03	1.21	2
6	0.7081E-05	1.85	0.3546E-03	1.04	2
7	0.1577E-05	2.17	0.1783E-03	0.99	5
8	0.3816E-06	2.05	0.8951E-04	0.99	8

In Table 10, we compute the P_2 conforming VEM solutions for (77) on the pentagonal meshes shown in Fig. 3. As on hexagonal meshes, the P_2 conforming VEM here converges at the optimal order in both norms. Comparing to Table 2, the pentagonal P_2 conforming VEM is much worse. But it has 1/3 less local degrees of freedom than that of P_2 hexagonal VEM.

In Table 11, we compute the P_3 conforming VEM solutions for (77) on the pentagonal meshes shown in Fig. 3. As on hexagonal meshes, the P_3 conforming VEM here converges at the optimal order only in H^1 norm. It converges half an order sub-optimal in L^2 norm. As pointed out earlier, it is likely due to the singularity that the exact solution (77) is only in $H^{3.5-\epsilon}(\Omega)$. The same orders of convergence will happen to the P_4 and P_5 VEM, as it happens to the hexagonal P_4 and P_5 VEM, in Tables 4 and 5. We would not repeat this computation. Instead, we will compute a smoother exact solution in Tables 12, 13 and 14.



Table 10 The error profile for (77) on meshes shown in Fig. 3, by the P_2 conforming VEM

Grid	$ u-u_h _0$	$O(h^r)$	$\ \nabla_h(u-u_h)\ _0$	$O(h^r)$	# Iter
1	0.8099E-02	0.00	0.5384E-01	0.00	1
2	0.7178E-03	3.50	0.1179E-01	2.19	1
3	0.8386E-04	3.10	0.2772E-02	2.09	2
4	0.9633E-05	3.12	0.6658E-03	2.06	2
5	0.1218E-05	2.98	0.1647E-03	2.02	5
6	0.1475E-06	3.05	0.4100E-04	2.01	7
7	0.1855E-07	2.99	0.1024E-04	2.00	9

Table 11 The error profile for (77) on meshes shown in Fig. 3, by the P_3 conforming VEM

Grid	$ u-u_h _0$	$O(h^r)$	$\ \nabla_h(u-u_h)\ _0$	$O(h^r)$	# Iter
1	0.6932E-02	0.00	0.5593E-01	0.00	1
2	0.4317E-03	4.01	0.6980E-02	3.00	1
3	0.2365E-04	4.19	0.8067E-03	3.11	2
4	0.2867E-05	3.04	0.1104E-03	2.87	3
5	0.2521E-06	3.51	0.1374E-04	3.01	6
6	0.2231E-07	3.50	0.1715E-05	3.00	9
7	0.1980E-08	3.49	0.2143E-06	3.00	12

To get a smoother solution, we choose the right-hand side function in (76) as

$$f = \frac{(1-2x)^3}{16} (4x^4 + 84x^2y^2 - 8x^3 - 84xy^2 + 5x^2 + 11y^2 - x + f_1),$$
where $f_1 = \begin{cases} -84x^2y + 84xy - 11y, & \text{if } x \le 1/2, \\ -168x^2y + 168xy - 22y, & \text{if } x > 1/2, \end{cases}$

we would get the exact solution u of (76) as

$$u = x(1-x)\left(x - \frac{1}{2}\right)^5 y u_1,$$
where $u_1 = \begin{cases} 1 - y, & \text{if } x \le 1/2, \\ 2 - y, & \text{if } x > 1/2. \end{cases}$ (80)

The solution is in $H^{5.5-\epsilon}(\Omega)$.

In Table 12, we compute the P_3 conforming VEM solutions again on the pentagonal meshes shown in Fig. 3, but for approximating a smoother exact solution (80). This time, the P_3 pentagonal conforming VEM converges at the optimal order in both H^1 norm and L^2 norm. This example shows that the finite element solution can converge at very high order as long as the exact solution is sufficiently smooth. But in theory, the L^2 order of convergence is limited to one and a half as the solution of the dual problem is limited to $H^{3/2}(\Omega)$.

In Table 13, we compute the P_4 conforming VEM solutions on the pentagonal meshes shown in Fig. 3, when approximating the smoother exact solution (80). The P_4 pentagonal conforming VEM converges at the optimal order in both H^1 norm and L^2 norm. Here the L^2 order of convergence looks like an half order super-convergence. But it was caused by fixed meshes and jumping of discrete boundary conditions on mesh points. The low-order



Table 12 The error profile for (80) on meshes shown in Fig. 3, by the P_3 conforming VEM

Grid	$ u - u_h _0$	$O(h^r)$	$\ \nabla_h(u-u_h)\ _0$	$O(h^r)$	# Iter
1	0.8712E-02	0.00	0.5175E-01	0.00	1
2	0.4041E-03	4.43	0.5095E-02	3.34	1
3	0.2430E-04	4.06	0.5899E-03	3.11	1
4	0.1273E-05	4.25	0.6752E-04	3.13	2
5	0.7213E-07	4.14	0.8249E-05	3.03	7
6	0.4539E-08	3.99	0.1023E-05	3.01	12
7	0.2830E-09	4.00	0.1276E-06	3.00	14

Table 13 The error profile for (80) on meshes shown in Fig. 3, by the P_4 conforming VEM

Grid	$\ u-u_h\ _0$	$O(h^r)$	$\ \nabla_h(u-u_h)\ _0$	$O(h^r)$	# Iter
1	0.6080E-02	0.00	0.3742E-01	0.00	1
2	0.1240E-03	5.62	0.2278E-02	4.04	1
3	0.3345E-05	5.21	0.1319E-03	4.11	2
4	0.9866E-07	5.08	0.7886E-05	4.06	4
5	0.1880E-07	2.39	0.6123E-06	3.69	6
6	0.4370E-09	5.43	0.3247E-07	4.24	11
7	0.1001E-10	5.45	0.1926E-08	4.08	15

Table 14 The error profile for (80) on meshes shown in Fig. 3, by the *P*₅ conforming VEM

Grid	$ u-u_h _0$	$O(h^r)$	$\ \nabla_h(u-u_h)\ _0$	$O(h^r)$	# Iter
1	0.2550E-02	0.00	0.1755E-01	0.00	1
2	0.2992E-04	6.41	0.5914E-03	4.89	1
3	0.4385E-06	6.09	0.1772E-04	5.06	2
4	0.9907E-08	5.47	0.5676E-06	4.96	6
5	0.2043E-09	5.60	0.1766E-07	5.01	11
6	0.4365E-11	5.55	0.5512E-09	5.00	15

approximation on Grid 5, in Table 13, raises the convergence orders at next two levels. In general, the L^2 order of convergence is 5.

In Table 14, finally we compute the P_5 conforming VEM solutions on the pentagonal meshes shown in Fig. 3, when approximating the smoother exact solution (80). The P_5 pentagonal conforming VEM converges at the optimal order in H^1 norm only, and at half an order sub-optimal in L^2 norm. The situation appears several times before. Here the exact solution is in $H^{5.5}(\Omega)$ which explains the 5.5 L^2 order of convergence.

6 Conclusions

We have proposed and analyzed conforming and nonconforming VEMs for the Signorini problems. Detailed a priori error estimates for lowest order schemes k=1 have been established. Extending the analysis to higher schemes k>1 and developing the corresponding posteriori indicators are challenging topics, that shall be carefully addressed in future work.



Acknowledgements The authors thank two anonymous referees for their valuable comments and suggestions which helped to improve the quality of this article.

Author Contributions All authors made equal contribution.

Funding The work of Y. Zeng is supported in part by the Guangdong Basic and Applied Basic Research Foundation (No. 2020A1515011032). The work of L. Zhong is supported in part by the National Natural Science Foundation of China (No. 12071160). The work of M. Cai is supported in part by NIH-RCMI grant through U54MD013376, and the National Science Foundation awards (1831950). The work of F. Wang is supported in part by the National Natural Science Foundation of China (Nos. 12071227 and 11871281), the National Key Research and Development Program of China 2020YFA0713803, and the Natural Science Foundation of the Jiangsu Higher Education Institutions of China 20KJA110001.

Data Availability Data sharing is not applicable to this article since no datasets were generated or collected in the work.

Declarations

Conflict of interest All authors declare that they have no potential Conflict of interest.

Compliance with Ethical Standards The submitted work is original and is not published elsewhere in any form or language. This article does not contain any studies involving animals. This article does not contain any studies involving human participants.

References

- Antonietti, P.F., Beirão Da Veiga, L., Scacchi, S., Verani, M.: A C¹ virtual element method for the Cahn-Hilliard equation with polygonal meshes. SIAM J. Numer. Anal. 54, 34–56 (2016)
- Antonietti, P.F., Manzini, G., Verani, M.: The fully nonconforming virtual element method for biharmonic problems. Math. Models Methods Appl. Sci. 28, 387–407 (2018)
- Arnold, D.N., Brezzi, F., Cockburn, B., Marini, L.D.: Unified analysis of discontinuous Galerkin methods for elliptic problems. SIAM J. Numer. Anal. 39, 1749–1779 (2002)
- Ayuso de Dios, B., Lipnikov, K., Manzini, G.: The nonconforming virtual element method. ESAIM Math. Model. Numer. Anal. 50, 879–904 (2016)
- Banz, L., Stephan, E.P.: A posteriori error estimates of hp-adaptive IPDG-FEM for elliptic obstacle problems. Appl. Numer. Math. 76, 76–92 (2014)
- Beirão da Veiga, L., Brezzi, F., Cangiani, A., Manzini, G., Marini, L.D., Russo, A.: Basic principles of virtual element methods. Math. Models Methods Appl. Sci. 23, 199–214 (2013)
- Beirão da Veiga, L., Lovadina, C., Russo, A.: Stability analysis for the virtual element method. Math. Models Methods Appl. Sci. 27, 2557–2594 (2017)
- Beirão da Veiga, L., Brezzi, F., Marini, L.D.: Virtual elements for linear elasticity problems. SIAM J. Numer. Anal. 51, 794–812 (2013)
- Belhachmi, Z., Ben Belgacem, F.: Quadratic finite element approximation of the Signorini problem. Math. Comput. 72, 83–104 (2001)
- Ben Belgacem, F.: Numerical simulation of some variational inequalities arisen from unilateral contact problems by the finite element method. SIAM J. Numer. Anal. 37, 1198–1216 (2000)
- Benedetto, M.F., Berrone, S., Pieraccini, S., Scialò, S.: The virtual element method for discrete fracture network simulations. Comput. Methods Appl. Mech. Engrg. 280, 135–156 (2014)
- Brenner, S.C., Scott, L.R.: The Mathematical Theory of Finite Element Methods, 3rd edn. Springer-Verlag, New York (2008)
- Brenner, S.C., Sung, L.Y.: Virtual element methods on meshes with small edges or faces. Math. Models Methods Appl. Sci. 28, 1291–1336 (2018)
- Brezzi, F., Hager, W.W., Raviart, P.A.: Error estimates for the finite element solution of variational inequalities, Part I: primal theory. Numer. Math. 28, 431–443 (1977)
- Brezzi, F., Marini, L.D.: Virtual element methods for plate bending problems. Comput. Methods Appl. Mech. Eng. 253, 455–462 (2013)



- 16. Bustinza, R., Sayas, F.J.: Error estimates for an LDG method applied to Signorini type problems. J. Sci. Comput. 52, 322-339 (2012)
- 17. Bürger, R., Kumar, S., Mora, D., Verma, N.: Virtual element methods for the three-field formulation of time-dependent linear poroelasticity. Adv. Comput. Math. 47, 2 (2021)
- 18. Cangiani, A., Georgoulis, E.H., Houston, P.: hp-Version discontinuous Galerkin methods on polygonal and polyhedral meshes. Math. Models Methods Appl. Sci. 24, 2009–2041 (2014)
- 19. Cangiani, A., Gyrya, V., Manzini, G.: The nonconforming virtual element method for the Stokes equations. SIAM J. Numer. Anal. 54, 3411-3435 (2016)
- 20. Cáceres, E., Gatica, G.N., Sequeira, F.A.: A mixed virtual element method for the Brinkman problem. Math. Models Methods Appl. Sci. 27, 707–743 (2017)
- 21. Cao, S., Chen, L.: Anisotropic error estimates of the linear virtual element method on polygonal meshes. SIAM J. Numer. Anal. 56, 2913–2939 (2018)
- 22. Cao, S., Chen, L.: Anisotropic error estimates of the linear nonconforming virtual element methods. SIAM J. Numer. Anal. 57, 1058–1081 (2019)
- 23. Cao, S., Chen, L., Guo, R., Lin, F.: Immersed virtual element methods for elliptic interface problems in two dimensions. J. Sci. Comput. **93**, 12 (2022)
- 24. Carstensen, C., Köhler, K.: Nonconforming FEM for the obstacle problem. IMA J. Numer. Anal. 37, 64-93 (2017)
- 25. Cascavita, K.L., Chouly, F., Ern, A.: Hybrid high-order discretizations combined with Nitsche's method for Dirichlet and Signorini boundary conditions. IMA J. Numer. Anal. 40, 2189-2226 (2020)
- 26. Chen, L., Wang, F.: A divergence free weak virtual element method for the Stokes problem on polytopal meshes. J. Sci. Comput. 78, 864–886 (2019)
- 27. Cicuttin, M., Ern, A., Gudi, T.: Hybrid high-order methods for the elliptic obstacle problem. J. Sci. Comput. 83, 1–18 (2020)
- 28. Di Pietro, D.A., Ern, A.: Mathematical Aspects of Discontinuous Galerkin Methods, vol. 69. Springer-Verlag, Berlin (2012)
- 29. Di Pietro, D.A., Ern, A.: A hybrid high-order locking-free method for linear elasticity on general meshes. Comput. Methods Appl. Mech. Eng. 283, 1–21 (2015)
- 30. Djoko, J.K.: Discontinuous Galerkin finite element methods for variational inequalities of first and second kinds. Numer. Methods PDEs. 24, 296-311 (2008)
- 31. Drouet, G., Hild, P.: Optimal convergence for discrete variational inequalities modelling Signorini contact in 2D and 3D without additional assumptions on the unknown contact set. SIAM J. Numer. Anal. 53, 1488–1507 (2015)
- 32. Falk, R.S.: Error estimates for the approximation of a class of variational inequalities. Math. Comput. 28, 963-971 (1974)
- 33. Feng, F., Han, W., Huang, J.: Virtual element methods for elliptic variational inequalities of the second kind. J. Sci. Comput. **80**, 60–80 (2019)
- 34. Frittelli, M., Sgura, I.: Virtual element method for the Laplace Beltrami equation on surfaces. ESAIM Math. Model. Numer. Anal. 52, 965-993 (2018)
- 35. Gardini, F., Manzini, G., Vacca, G.: The nonconforming virtual element method for eigenvalue problems. ESAIM Math. Model. Numer. Anal. 53, 749-774 (2019)
- 36. Gardini, F., Vacca, G.: Virtual element method for second order elliptic eigenvalue problems. IMA J. Numer. Anal. 38, 2026–2054 (2018)
- 37. Glowinski, R.: Numerical Methods for Nonlinear Variational Problems. Springer-Verlag, Berlin (2008)
- 38. Guan, O., Gunzburger, M., Zhao, W.: Weak-Galerkin finite element methods for a second-order elliptic variational inequality. Comput. Methods Appl. Mech. Engrg. 337, 677–688 (2018)
- 39. Gudi, T., Kamana, P.: A posteriori error control of discontinuous Galerkin methods for elliptic obstacle problems. Math. Comput. 83, 579–602 (2014)
- 40. Han, W., Wang, L.: Nonconforming finite element analysis for a plate contact problem. SIAM J. Numer. Anal. 40, 1683–1697 (2002)
- 41. Herbin, R.: A monotonic method for the numerical solution of some free Boundary value problems. SIAM J. Numer. Anal. **40**, 2292–2310 (2002)
- 42. Hild, P., Renard, Y.: An improved a priori error analysis for finite element approximations of Signorini's problem. SIAM J. Numer. Anal. 50, 2400–2419 (2012)
- 43. Hua, D., Wang, L.: The nonconforming finite element method for Signorini problem. J. Comput. Math. **25**, 67–80 (2007)
- 44. Kikuchi, N., Oden, J.T.: Contact Problems in Elasticity: A Study of Variational Inequalities and Finite Element Methods. SIAM, Philadelphia (1988)
- 45. Kinderlehrer, D., Stampacchia, G.: An Introduction to Variational Inequalities and Their Applications. Academic Press, New York (1980)



46. Lemaire, S.: Bridging the hybrid high-order and virtual element methods. IMA J. Numer. Anal. 41, 549-593 (2021)

(2024) 100:18

- 47. Mu, L., Wang, X., Wang, Y.: Shape regularity conditions for polygonal/polyhedral meshes, exemplified in a discontinuous Galerkin discretization. Numer. Methods PDEs 31, 308–325 (2015)
- 48. Shi, D., Ren, J., Gong, W.: Convergence and superconvergence analysis of a nonconforming finite element method for solving the Signorini problem. Nonlinear Anal. Real World Appl. 75, 3493–3502 (2012)
- 49. Shi, D., Xu, C.: EO_1^{rot} nonconforming finite element approximation to Signorini problem. Sci. China Math. **56**, 1301–1311 (2013)
- 50. Tang, X., Liu, Z., Zhang, B., Feng, M.: On the locking-free three-field virtual element methods for Biot's consolidation model in poroelasticity. ESAIM Math. Model. Numer. Anal. 55, 909–939 (2021)
- 51. Wang, F., Han, W., Cheng, X.: Discontinuous Galerkin methods for solving elliptic variational inequalities. SIAM J. Numer. Anal. 48, 708–733 (2010)
- 52. Wang, F., Han, W., Cheng, X.: Discontinuous Galerkin methods for solving the Signorini problem. IMA J. Numer. Anal. 31, 1754–1772 (2011)
- 53. Wang, F., Reddy, B.D.: A priori error analysis of virtual element method for contact problem. Fixed Point Theory Algorithms Sci. Eng. **2022**, 10 (2022)
- 54. Wang, F., Wei, H.: Virtual element methods for the obstacle problem. IMA J. Numer. Anal. 40, 708–728 (2020)
- 55. Wang, F., Wu, B., Han, W.: The virtual element method for general elliptic hemivariational inequalities. J. Comput. Appl. Math. 389, 113330 (2021)
- 56. Wang, F., Zhao, J.: Conforming and nonconforming virtual element methods for a Kirchhoff plate contact problem. IMA J. Numer. Anal. 41, 1458–1483 (2021)
- 57. Wang, G., Mu, L., Wang, Y., He, Y.: A pressure-robust virtual element method for the Stokes problem. Comput. Methods Appl. Mech. Eng. 382, 113879 (2021)
- 58. Wang, J., Ye, X.: A weak Galerkin finite element method for second-order elliptic problems. J. Comput. Appl. Math. **241**, 103–115 (2013)
- 59. Wang, L.: On the quadratic finite element approximation to the obstacle problem. Numer. Math. 92, 771-778 (2002)
- 60. Wang, L.: On the error estimate of nonconforming finite element approximation to the obstacle problem. J. Comput. Math. **21**, 481–490 (2003)
- 61. Wei, H., Huang, X., Li, A.: Piecewise divergence-free nonconforming virtual elements for Stokes problem in any dimensions. SIAM J. Numer. Anal. 59, 1835–1856 (2021)
- 62. Zeng, Y., Chen, J., Wang, F.: Error estimates of the weakly over-penalized symmetric interior penalty method for two variational inequalities. Comput. Math. Appl. 69, 760–770 (2015)
- 63. Zhang, S.: Coefficient jump-independent approximation of the conforming and nonconforming finite element solutions. Adv. Appl. Math. Mech. 8, 722–736 (2016)
- 64. Zhao, J., Chen, S., Zhang, B.: The nonconforming virtual element method for plate bending problems. Math. Models Methods Appl. Sci. 26, 1671–1687 (2016)
- 65. Zhao, J., Mao, S., Zhang, B., Wang, F.: The interior penalty virtual element method for the biharmonic problem. Math. Comput. 920, 1543–1574 (2023)
- 66. Zhao, J., Zhang, B., Mao, S., Chen, S.: The divergence-free nonconforming virtual element for the Stokes problem. SIAM J. Numer. Anal. 57, 2730–2759 (2019)

Publisher's Note Springer Nature remains neutral with regard to jurisdictional claims in published maps and institutional affiliations.

Springer Nature or its licensor (e.g. a society or other partner) holds exclusive rights to this article under a publishing agreement with the author(s) or other rightsholder(s); author self-archiving of the accepted manuscript version of this article is solely governed by the terms of such publishing agreement and applicable

